First Scanning Doppler Imager Observations of the 843 nm Mesopheric OH Emission

M. Conde,[1] M. Singh Dhadly[1], C. Anderson[1], M. G. McHarg,[2] M. Kosch,[3] R.W. Smith[1], C Andersen[1] [[1]GI-UAF; [2]US Air Force Academy; [3]Lancaster University]

Geophysical Institute
University of Alaska Fairbanks

LANCASTER UNIVERSITY

Abstract

The "Scanning Doppler Imager" technique has been used since the mid 1990's to measure thermospheric wind fields – first at Poker Flat in Alaska [*Conde & Smith*, 1995, and more recently also at Mawson (Antarctica) [*Anderson et al.*, 2009], Longyearbyen (Svalbard) [*Griffin et al.*, 2008], and Gakona (Alaska) [*Anderson et al.*, 2012a]. However, all published data have so far been derived from observing emissions at either 630 nm or 558 nm, both of which come from atomic oxygen and, in the auroral zone, both are emitted primarily in the thermosphere. Here we report on the first ever application of the technique to measuring mesopause wind and temperature fields using OH emissions that originate from a layer at a height of around 86 km ±1 km. During the recent 2011-2012 observing season we installed an 843 nm OH filter, on loan from Lancaster University in the UK, into the US Air Force Academy's all-sky imaging Fabry-Perot spectrometer at Gakona in Alaska. The instrument was programmed to include the OH filter in its normal observing cycle – which also included 630 nm and 558 nm oxygen emissions and, when the aurora was bright, the O^+ 732 nm emission as well. The all-sky field of view at 843 nm was resolved into 43 sub-fields, which required integration times of around 10 min to achieve good signal/noise ratio spectra. We report here on results from the first 6 months of these OH observations.

The Air Force Academy SDI

In the mid 1990's the University of Alaska's Geophysical Institute developed a new type of Fabry-Perot spectrometer for remote sensing thermospheric wind and temperature fields. Installed at Poker Flat in Alaska and dubbed the "Scanning Doppler Imager" (SDI), its salient features included a low-light imaging detector with high time resolution, a capacitance-stabilized etalon capable of piezo-electric separation scanning at 10 Hz or faster, and wide-angle fore optics arranged to place a sharp image of the sky onto the detector [*Conde & Smith*, 1995, 1997, 1998]. The instrument resolves the sky scene into a software-defined set of sub-regions, and compiles a high-resolution Doppler spectrum of the source illumination originating from each one. These spectra are then used to infer two-dimensional maps of vector wind and scalar temperature at the height of the atmospheric optical emission layer.

In 2009 the University of Alaska constructed a new SDI for the US Air Force Academy, and installed it at the site of the HAARP facility at Gakona, Alaska. Figure 1 shows the instrument and the trailer that houses it. This instrument has been used very successfully in conjunction with a similar one at Poker Flat to infer F-region wind fields using bistatic Doppler spectroscopy [*Anderson et al.*, 2012 a, b, & c].

***Figure 1**: (Top) A fish-eye lens view of the US Air Force Academy Scanning Doppler Imager, and the University of Alaska Trailer that houses it at the HAARP site (bottom).*

First Observations of Mesospheric OH

Until the northern Fall of 2011, all observations by the AFA-SDI had been conducted at wavelengths of either 630 nm or 558 nm. For the most part this is also true of the other three existing SDI instruments, the only exception being that we do currently have a number of years of (unpublished) twilight spectra of sunlight resonantly scattered at 589 nm by mesospheric sodium. In early November of 2011 two of us (Smith & Andersen) installed additional filters in the AFA instrument, to allow observations of the mesospheric OH emission at 843 nm, and of the thermospheric O^+ emission at 732 nm. The software that runs the SDI allows very flexible observing modes. We initially programmed the AFA instrument to take 732 nm spectra at twilight and, during full darkness, to interleave single 843 nm exposures between two pairs of observations at 630 nm and 558 nm.

However, we soon learned that auroral light leaks through the 843 nm filter during bright auroral displays, resulting in erroneously high inferred temperatures and distorted wind fields. We therefore modified the observing script to replace the scheduled 843 nm observations with alternate ones at 732 nm whenever the 558 nm emission brightness exceed its typical quiescent level. The instrument is thus able to respond autonomously to changing auroral activity, and make observations that are most appropriate for the prevailing conditions.

The purpose of this poster is to present a survey of results obtained during this first winter of OH observations. These results are not definitive; they are very much a "first look".

Basic Data

Figure 2 shows an example of the original spectra obtained during one 10-minute exposure at 843 nm, centered on 05:57 UT on the night of December 22, 2011. It is a sky map view, so the center of the image corresponds to looking in the zenith, and radial distance in the image maps linearly to zenith angle. The outer edge of the image circle is at roughly 80° zenith angle. White and orange curves show, for each of the 43 observing zones, the OH sky spectra and the instrumental wavelength passband. The background red, blue, and purple hues indicate the Doppler temperature inferred in each zone. Yellow arrows indicate the inferred horizontal vector wind at the location of each zone, scaled according the the calibration arrow shown in the lower right.

Typical OH emission brightness is only ~ 500 Rayleighs, which is much dimmer than that of either the 630 nm or 558 nm at most times for these auroral latitudes, especially under the current pre solar-maximum conditions. Further, the camera quantum efficiency at 843 nm is only ~ 50% , which which is significantly less than the ~ 90% efficiency that it achieves throughout the visible band. Because of this, the OH observations require longer exposures (10 minutes, versus only a few minutes for 630 nm or 558 nm spectra), and we were not able to divide the field of view into as many zones (43 versus 115, typically). Even then, the signal/noise ratio achieved in the OH spectra is well below that of the other two emissions. Nevertheless, it is adequate to provide geophysically useful wind and temperature estimates, as we show here.

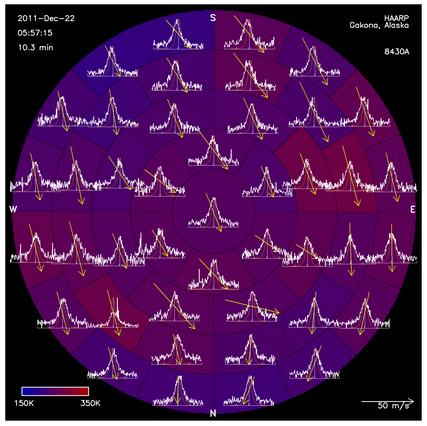

***Figure 2**: OH sky spectra, taken at 05:57 UT on the night of December 22, 2011, as described in the text.*

Examples of Time Series Data

Figure 3 shows a time series of temperatures obtained on the night of December 22, 2011. The single value shown at each time corresponds to the median temperature calculated from all 43 zones that contribute to a single exposure. "Error bars" denote the range spanned by ± one standard deviation of the 43 temperature estimates obtained from each exposure. Colored curves denote MSIS temperatures calculated for various heights (as indicated) using the A_p and $F_{10.7}$ index values prevailing at the time.

As indicated in Figure 3, the 843 nm Doppler temperature estimates tend to be somewhat higher than the corresponding MSIS values for the expected emission height of 86 km. Several factors may contribute to this. Firstly, it is likely that auroral leakage never completely goes to zero at these latitudes, in which case all our spectra would be slightly broadened by a low level contaminant emission. Secondly, the OH emission is actually a hyperfine doublet, which would normally require a Doppler fitting procedure that could account for both components. Here, however, we have used an etalon with a gap of 18.6 mm, which should cause the the interference order of the two components of the doublet to differ by exactly one at any given incidence angle. Theoretically, this means the two components should appear exactly superimposed in our spectra, so that no special procedure would be needed to account for the doublet. However, if the overlap is imperfect for some reason, this would broaden the spectra and could produce the slightly elevated temperature estimates that we obtain. (We have not yet tested this hypothesis; we merely note here that it is a possibility.)

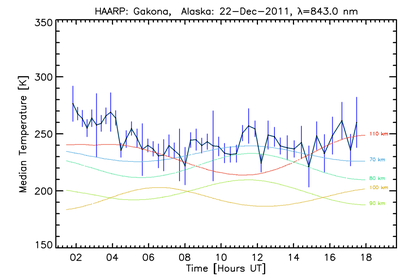

***Figure 3**: All-sky median temperature estimates obtained from OH spectra recorded on the night of December 22, 2011, as described in the text.*

Figure 4 shows time series of the zonal and meridional wind components above Gakona for the night of December 22, 2011. In this case the directions are defined to be parallel to magnetic east and north respectively, where "magnetic" directions are oriented such that east is parallel to the statistical orientation of the auroral oval at this location, and north is perpendicular to it. Winds shown at each time in Figure 4 are spatial averages over the entire field of view. We have not yet compared these winds with expectations from models.

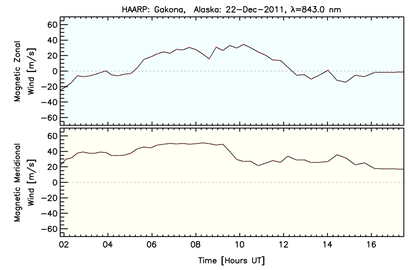

***Figure 4**: Estimates of the magnetic zonal and meridional components of the horizontal wind, obtained from OH spectra recorded on the night of December 22, 2011.*

Figure 5 shows time series of vertical wind, together with the divergence and vorticity of the horizontal wind above Gakona for the night of December 22, 2011. The vertical wind and divergence time series are strongly suggestive of a monochromatic gravity wave, although the vertical wind amplitude seems rather large for 86 km altitude.

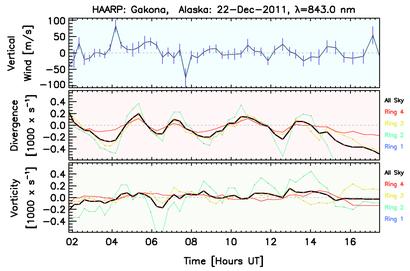

***Figure 5**: Estimates of the vertical wind together with the divergence and vorticity of the horizontal wind, obtained from OH spectra recorded on the night of December 22, 2011.*

Two-Dimensional Temperature and Wind Fields

The left panel of Figure 6 shows sky maps of the Doppler temperature inferred from OH spectra obtained on the night of December 22, 2011. There was no significant aurora above Gakona on this night, so the (weak) spatial structures seen in the temperature maps are unlikely to be due to auroral contamination.

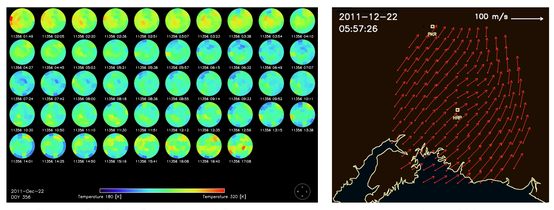

***Figure 6**: (Left) Sky maps of Doppler temperature, obtained from OH spectra recorded on the night of December 22, 2011. (Right) An example of the spatially resolved horizontal vector wind field at mesopause heights, projected onto a geographic map of Alaska.*

The right panel of Figure 6 shows one example of an inferred two-dimensional horizontal vector wind field, projected onto a map of Alaska. These data are from the same time as Figure 2, but in this case the wind field is mapped geographically (whereas in Figure 2 it is shown as a sky view.) Note also that the geographic projection program has over-sampled the wind field at a somewhat higher spatial resolution than that defined by the original data. (The spatial resolution is chosen by the program to be appropriate for 630 nm or 558 nm data, which are recorded in 115 zones, instead of the 43 zones used during OH observations.)

Whole-Season Periodograms

Figure 7 shows periodograms of 843 nm wind data calculated over the entire 2011/2012 season. Figure 8, shown for comparison, is a similar presentation of 558 nm wind periodograms. Data from periods of very heavy cloud have been removed in each case. Zonal winds at both heights developed significant power at periods of 15 to 25 days during January and early February, possibly due to planetary wave activity. (No similar feature appears in periodograms of the A_p or $F_{10.7}$ indices during this time interval.)

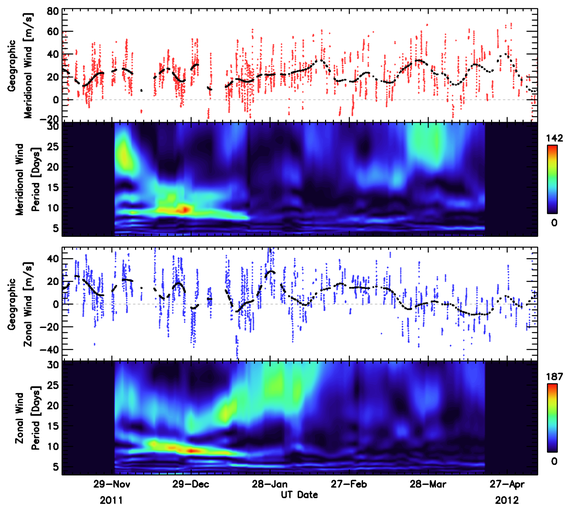

***Figure 7**: The top panel shows estimates of the geographic meridional wind component derived from 843 nm OH spectra for the entire 2011-2012 winter data set. The second panel shows dynamic spectra (periodograms) of these data calculated using the Lomb-Scargle algorithm applied over a 40-day sliding window. The bottom two panels are the same as the top two, except that they show data for the geographic zonal wind component.*

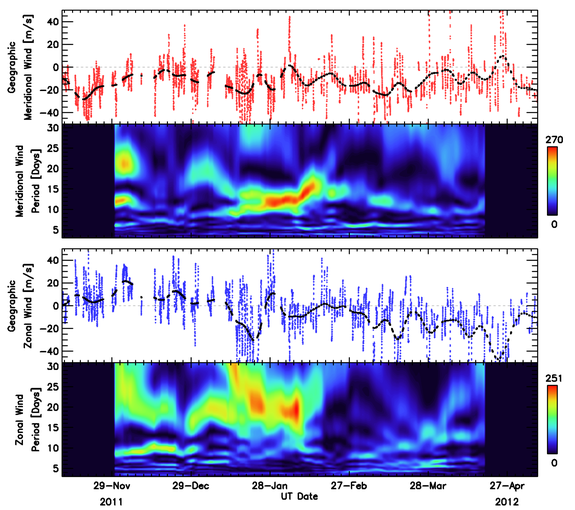

***Figure 8**: As for Figure 7, but in this case showing data for the 558 nm emission from lower thermospheric atomic oxygen.*

Conclusions

The SDI instrument does appear able to produce useful spatially-resolved estimates of mesopause wind and temperature fields, based on Doppler spectra of the 843 nm OH emission. All data are preliminary, and will require considerable validation before they could be used routinely. However, if successfully validated, this could be a promising new technique for studying mesospheric dynamics. It probably offers most potential at middle and low latitudes, where auroral contamination would not be a problem.

References: Anderson et al. (2009), *Ann. Geophys.*, 27, 2225-2235; Anderson et al. (2012a), *JGR*, 117, A03304, doi:10.1029/2011JA017041; Anderson et al. (2012b), *JGR*, 117, A03305, doi:10.1029/2011JA017157; Anderson et al. (2012c) *JGR* doi:10.1029/2011JA017471, in press; Conde, M. & R. Smith (1995), *GRL*, 22, 3019-3022; Conde, M & R. Smith (1997), *Appl. Opt.*, 36, 5441-5450; Conde, M. & R.Smith (1998), *JGR*, 103, 9449-9471; Griffin et al. (2008), *Ann. Geophys.*, 26, 2649-2655;